JACS
JOURNAL OF THE AMERICAN CHEMICAL SOCIETY

Communication

pubs.acs.org/JACS

Route to the Smallest Doped Semiconductor: Mn^{2+}-Doped $(CdSe)_{13}$ Clusters

Jiwoong Yang,[†,‡,▽] Rachel Fainblat,[§,▽] Soon Gu Kwon,[†,‡] Franziska Muckel,[§] Jung Ho Yu,[†,‡] Hendrik Terlinden,[§] Byung Hyo Kim,[†,‡] Dino Iavarone,[§] Moon Kee Choi,[†,‡] In Young Kim,[∥] Inchul Park,[†,⊥] Hyo-Ki Hong,[#] Jihwa Lee,[†,‡] Jae Sung Son,[#] Zonghoon Lee,[#] Kisuk Kang,[†,⊥] Seong-Ju Hwang,[∥] Gerd Bacher,*[,§] and Taeghwan Hyeon*[,†,‡]

[†]Center for Nanoparticle Research, Institute for Basic Science (IBS), Seoul 151-742, Republic of Korea

[‡]School of Chemical and Biological Engineering and [⊥]Department of Materials Science and Engineering, Seoul National University, Seoul 151-742, Republic of Korea

[§]Werkstoffe der Elektrotechnik und CENIDE, Universität Duisburg-Essen, 47057 Duisburg, Germany

[∥]Materials Research Institute for Clean Energy, Department of Chemistry and Nano Sciences, Ewha Womans University, Seoul 120-750, Republic of Korea

[#]School of Materials Science and Engineering, Ulsan National Institute of Science and Technology, Ulsan 689-798, Republic of Korea

Supporting Information

ABSTRACT: Doping semiconductor nanocrystals with magnetic transition-metal ions has attracted fundamental interest to obtain a nanoscale dilute magnetic semiconductor, which has unique spin exchange interaction between magnetic spin and exciton. So far, the study on the doped semiconductor NCs has usually been conducted with NCs with larger than 2 nm because of synthetic challenges. Herein, we report the synthesis and characterization of Mn^{2+}-doped $(CdSe)_{13}$ clusters, the smallest doped semiconductors. In this study, single-sized doped clusters are produced in large scale. Despite their small size, these clusters have semiconductor band structure instead of that of molecules. Surprisingly, the clusters show multiple excitonic transitions with different magneto-optical activities, which can be attributed to the fine structure splitting. Magneto-optically active states exhibit giant Zeeman splittings up to elevated temperatures (128 K) with large *g*-factors of 81(±8) at 4 K. Our results present a new synthetic method for doped clusters and facilitate the understanding of doped semiconductor at the boundary of molecules and quantum nanostructure.

For the last decades, the synthesis of semiconductor nanocrystals (NCs) has been rapidly developed from controlling the size[1] and shape[2] to designing various multicomponent heterostructures for synergetic combination of the quantum confinement effect with the tradition semiconductor technology such as heterojunction and doping. In particular, doping semiconductor NCs with magnetic transition metals have attracted substantial interests to obtain diluted magnetic semiconductor (DMS) NCs. Spin exchange interaction between the dopants and the charge carriers of the host in these NCs leads to unique correlated electronic and magnetic properties such as giant magneto-optical response. So far synthesis of various kinds of doped semiconductor NCs has been reported.[3−6] Despite the progress on the doping of semiconductor NCs, the study of doped semiconductor NCs is usually limited to NCs larger than 2 nm. Typically, doping of NCs is known to be induced by the adsorption of impurities on the surface of growing NCs.[6] Because this process requires the preformed NCs of certain sizes for adsorption of the dopant, there is almost no chance for the dopants to be incorporated into the very small-sized NCs. Thus, it is an open question whether doping of subnanometer-sized semiconductor is feasible at all.

Herein we report on the synthesis and characterization of the smallest doped semiconductor, Mn^{2+}-doped $(CdSe)_{13}$ clusters. It has been known that magic-sized CdSe clusters are formed transiently before the nucleation and growth of CdSe NCs.[7] By adjusting the reaction conditions, we successfully obtained single-sized $(CdSe)_{13}$ clusters doped with Mn^{2+} with 99% yield. Molecular formula of these clusters is $Cd_{13-x}Mn_xSe_{13}$ (x = 1, 2). This amounts to the doping concentration of 7.7 and 15.4% for x = 1 and 2, respectively, which is considerably high compared to the previously reported Mn^{2+}-doped CdSe NCs. Note that this high doping concentration by the introduction of a single dopant is directly related to the extremely small size of our clusters. Although the clusters have very small size, they have semiconductor band structure, which highlights them as the smallest doped semiconductors reported to date. Due to their small size, the clusters show multiple excitonic transitions with different magneto-optical activities, which might correspond to the fine structure states. Magneto-optically active states exhibit magneto-optical responses up to 128 K and a huge *g*-factor of 81(±8) at 4 K. This work demonstrates that subnanometer-sized doped clusters can be obtained, which represents magnetically doped semiconductors consisting of only 26 core atoms.

The synthesis of Mn^{2+}-doped $(CdSe)_{13}$ clusters is performed by adding selenocarbamate to a solution containing $CdCl_2$ and $MnCl_2$ in octylamine, which leads to the formation of octylamine

Received: July 28, 2015
Published: October 2, 2015

DOI: 10.1021/jacs.5b07888
J. Am. Chem. Soc. 2015, 137, 12776−12779

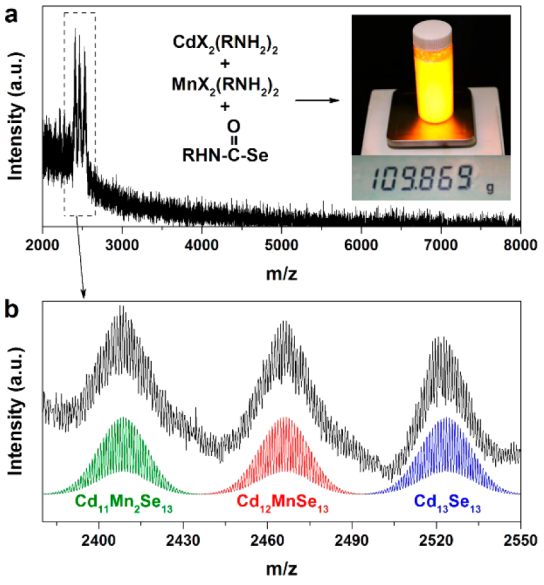

Figure 1. Synthesis of Mn^{2+}-doped $(CdSe)_{13}$ clusters. (a) Mass spectrum of Mn^{2+}-doped $(CdSe)_{13}$ clusters ionized with Cl^-. The average doping concentration of the clusters is 7%. The inset shows the amount of the product from a single batch large-scale synthesis. (b) High-resolution mass spectrum of the main peaks indicated with the dashed box in panel a. Below the measured data, calculated isotopic distributions of $Cd_{13}Se_{13}$ (blue), $Cd_{12}MnSe_{13}$ (red), and $Cd_{11}Mn_2Se_{13}$ (green) are shown for comparison.

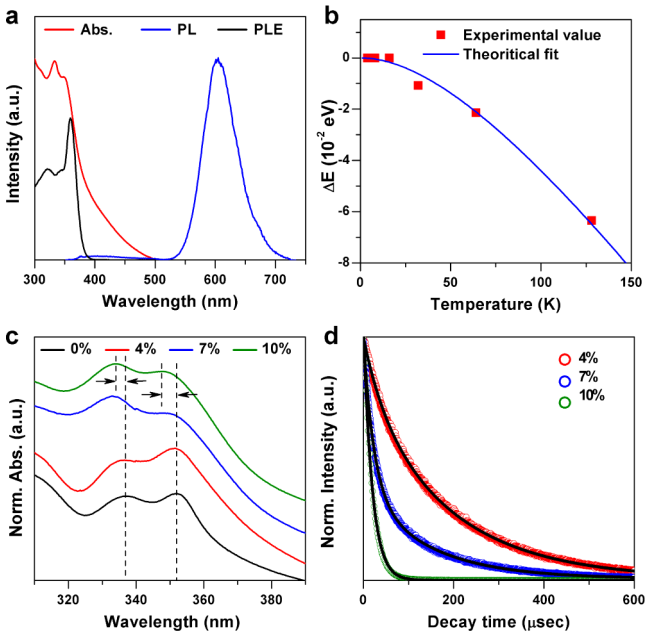

Figure 2. Optical properties of Mn^{2+}-doped $(CdSe)_{13}$ clusters. (a) Spectra of absorption, PL, and PLE (detected at 600 nm) from as-synthesized (*n*-octylamine capped) 7% Mn^{2+}-doped $(CdSe)_{13}$ clusters. (b) Energy shift of the absorption edge of Mn^{2+}-doped $(CdSe)_{13}$ clusters as a function of temperature. The theoretical fitting curve is calculated by using the Varshni law with the parameters $\alpha = 11 \times 10^{-4}$ eV K^{-1} and $\beta = 150$ K. (c) Absorption spectra of $(CdSe)_{13}$ clusters with various doping concentrations. The arrows indicate the shift of the absorption peak positions. (d) Time-resolved luminescence decay at 600 nm from Mn^{2+}-$(CdSe)_{13}$ clusters with different doping concentrations. Decay data are overlapped with the corresponding fitting curve (black).

capped CdSe clusters via Lewis acid–base reaction between the metal halide–amine complex and the selenium precursor.[2c,d] Further reaction to form CdSe NCs from the clusters is suppressed by lowering the reaction temperature to 25 °C. By changing the coordinating ligands, we can control the reaction kinetics or the dispersibility of the clusters (see the Supporting Information (SI)). The CdSe clusters obtained were analyzed by laser desorption/ionization time-of-flight (LDI-TOF) mass spectrometry (MS), and the result is shown in Figure 1. The three main peaks in the mass spectrum are unambiguously assigned to $Cd_{13}Se_{13}$, $Cd_{12}MnSe_{13}$, and $Cd_{11}Mn_2Se_{13}$ (Figure 1b). Other clusters such as $(CdSe)_{34}$ or $(CdSe)_{19}$ are not detected,[7f,g] confirming the high purity of the products. When no Mn precursor is added to the reaction solution, the clusters synthesized show only $Cd_{13}Se_{13}$ peak in the mass spectrum (Figure S1 in the SI). As a result, MS data confirm that $Cd_{13-x}Mn_xSe_{13}$ ($x = 1, 2$) are $(CdSe)_{13}$ clusters with one or two Cd^{2+} replaced with Mn^{2+}. Although there are only two kinds of Mn^{2+}-doped clusters with exact doping concentrations (7.7% and 15.4%), the *average* doping concentration (x_{Mn}) of the product from each synthesis is continuously increased from 0% to 10% with the amount of the Mn precursor in the solution (Figure S2 in the SI). This indicates that the molar ratio of $Cd_{13}Se_{13}$, $Cd_{12}MnSe_{13}$, and $Cd_{11}Mn_2Se_{13}$ clusters in the product is dependent on $[Mn^{2+}]$ in the reaction solution. Our method is very simple and reliable so that it can be easily scaled up to obtain more than 100 g from a single batch reaction in nearly quantitative yield (~99%, the inset of Figure 1a).[8]

The electronic energy structure of Mn^{2+}-doped $(CdSe)_{13}$ clusters was investigated by optical spectroscopy. In Figure 2a, absorption spectrum shows band edge excitonic transitions around 350 nm (3.54 eV), which is significantly blue-shifted from the band gap of bulk CdSe (1.75 eV) due to the strong quantum confinement. The absorption signal for the wavelength between 350 and 500 nm is influenced by scattering processes, which can be minimized by ligand exchange with long-chain unsaturated amines. In the photoluminescence (PL) spectrum, the band edge emission at 365 nm observed from undoped $(CdSe)_{13}$ clusters (see Figure S3 in the SI) is suppressed. Instead, an intense emission around 600 nm is observed, which is attributed to the internal ($^4T_1$-$^6A_1$) Mn^{2+} transition. Photoluminescence excitation (PLE) spectrum of this emission exhibits nearly the same transitions as the absorption spectrum, confirming the energy transfer from the host semiconductor band states to Mn^{2+} states. These data prove that Mn^{2+} is sitting in a Cd^{2+} site with tetrahedral site symmetry of the $(CdSe)_{13}$ hosts.[9] The shift between the maxima of PLE and absorption spectra can be attributed to different fine structure states contributing to each signal, as discussed below using magneto-optical studies. Interestingly, temperature-dependent shift of the absorption edge of Mn^{2+}-doped $(CdSe)_{13}$ clusters is well fitted with Varshni's law (Figure 2b). This suggests that these clusters have semiconductor band structure in spite of their extremely small size, which highlights them as the smallest doped inorganic semiconductor reported so far. As the average doping concentration is increased from 0% to 10%, the absorption peak position is shifted by ~43 meV, which is another evidence of doping that affects the band structure of the host (Figure 2c).[9b] In addition, as the doping concentration increases, the lifetime of internal ($^4T_1$-$^6A_1$) Mn^{2+} transition rapidly decreases (Figure 2d).[9b,c] For the clusters with the intermediate doping concentration of 7%, the decay curve fits well to a double exponential with $\tau_1 = 23$ μs and $\tau_2 = 143$ μs. On the other hand,

DOI: 10.1021/jacs.5b07888
J. Am. Chem. Soc. 2015, 137, 12776–12779

for 10% doped clusters, single exponential decay with τ = 19 μs gives the best fit (Figure S4 in the SI). This result suggests that $Cd_{12}MnSe_{13}$ and $Cd_{11}Mn_2Se_{13}$ have slow (>100 μs) and fast (<50 μs) decay rates, respectively, and that the statistical distribution of each species in an ensemble is changed according to the average doping concentration. The shortening of the decay time with increasing Mn concentration might indicate a partial lifting of the spin selection rules in exchange coupled Mn^{2+} pairs.[9c] Moreover, the lattice distortion caused by doping possibly increases nonradiative losses. This is supported by the trend that the quantum yield (QY) decreases with increasing average doping concentration: QY = 10%, 8%, and 6% for x_{Mn} = 4%, 7%, and 10%, respectively.

It is of fundamental interest whether doped clusters containing only 26 atoms can exhibit characteristics of magnetically doped semiconductors.[2d,5] A pronounced magnetic circular dichroism (MCD) signal is observed for the Mn^{2+}-doped clusters (Figure 3). This indicates a strong coupling between the charge carriers of the host material and the substitutional Mn^{2+}-dopants,[4b] proving the membership of this material to the family of DMS nanostructures. In our experiments the ground state in the absorption process (zero exciton) is a nondegenerate spin zero state[1a] and does not split in a magnetic field. Therefore, the resulting MCD signal is determined by the A term of the MCD signal and thus proportional to the first derivative of the absorbance. For that reason, the zero-crossing of the MCD spectrum should be located at the same energy as the absorption maximum. Indeed, this is usually observed for DMS.[4,5] Surprisingly, a different result is found in this work (Figure 3a). The number of zero-crossings suggests that the measured MCD signals consist of three different magneto-optically active transitions. Because of the mismatch between the energy positions of the MCD zero-crossings and the absorption maxima, there should be at least two magneto-optically inactive transitions.

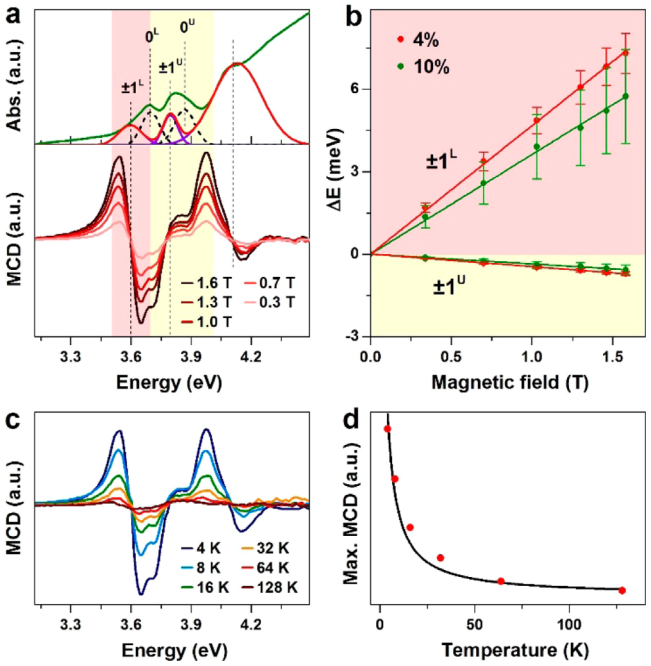

Figure 3. Magneto-optical properties of Mn^{2+}-doped $(CdSe)_{13}$ clusters. (a) Optical absorption (upper) and magnetic field-dependent MCD (lower) spectra of 4% Mn^{2+}-doped clusters at 4.2 K. In the upper panel, green, violet, and black dashed lines indicate measured data, magneto-optically active, and inactive peaks, respectively. The red curve is the summation of the magneto-optically active transitions. (b) Giant Zeeman splittings extracted from 4% (red) and 10% (green) Mn^{2+}-doped clusters. (c) Temperature-dependent MCD spectra of 4% Mn^{2+}-doped clusters under the magnetic field of 1.6 T. (d) Maximum amplitude of the MCD signal in panel c as a function of temperature. The black curve represents a theoretical Brillouin fit.

Indeed, we can resolve multiple excitonic transitions in the absorption spectrum (Figure 3a). Following the theoretical study of Efros et al.,[1a] the 8-fold degenerated band-edge energy level is expected to split into five sublevels, labeled by "new" quantum numbers ±2, $\pm1^L$, 0^L, $\pm1^U$, and 0^U. The magneto-optically active peaks at 3.60 and 3.79 eV might be related to the $\pm1^L$ and $\pm1^U$ states, respectively (violet lines in Figure 3a). The magneto-optically inactive transitions at 3.70 and 3.86 eV might involve $0^{L/U}$ states, which do not split under an external magnetic field (black dashed lines in Figure 3a). The low-energy contribution to the absorption signal at ~3.4 eV is possibly correlated to the ±2 state. Its contribution to the MCD signal, however, can be neglected, because of the selection rules and the low oscillator strength of this optically passive state. The optical transition around 4.1 eV involves upper excited states. It should be noted that the above notation of the fine structure split energy states is derived from a theoretical study based on the envelope function model,[1a] which means that quantitative details (e.g., exact energy levels) cannot be simply extrapolated toward these ultrasmall clusters. Independent from the limitations of the envelope function model, the occurrence of magneto-optically active and inactive transitions becomes obvious from our experimental data (Figure 3a and Figure S5 in the SI).

By excluding magneto-optically inactive transitions (see red curve in Figure 3a, where the new absorption maxima show the same energy as the MCD zero-crossings), we can extract the giant Zeeman splitting of Mn^{2+}-doped clusters (Figure 3b). The experimental values for the effective g-factor of the 4% Mn^{2+}-doped clusters are $81(\pm8)$ and $-8(\pm1)$ for the $\pm1^L$ and $\pm1^U$ states, respectively; those of the 10% Mn^{2+}-doped clusters are $63(\pm18)$ and $-6(\pm2)$ for the $\pm1^L$ and $\pm1^U$ states, respectively. These huge g-factors (at least 60 times greater than in the case of undoped CdSe nanocrystals)[10a] clearly indicate substantial exchange coupling between the localized 3d-electrons of the manganese and delocalized band charge carriers in the conduction and valence band. Note that the g-factors are still small compared to record data obtained on DMS nanocrystals, where the highest experimentally achieved g_{eff} is of order of 907[10b] (at 1.8 K and x_{Mn}= 29%, corresponding to a g_{eff} of ~390 at 4.2 K). In our studies we still have undoped clusters within an ensemble, which contribute to the total absorption but not to the magneto-optical activity, resulting in a reduction of the extracted Zeeman splitting. Moreover in the extremely small structures studied here, the quantum confinement is expected to affect both the spin−spin exchange interaction between the charge carriers and the dopants[2d,5b,c] as well as the valence-band mixing,[1a,10c] possibly leading to a decrease of the magneto-optical response. The 10% Mn^{2+}-doped clusters exhibit a slightly lower Zeeman splitting than the 4% doped ones. This result points to the formation of antiferromagnetically coupled Mn^{2+}−Mn^{2+} pairs in $Cd_{11}Mn_2Se_{13}$ clusters that are the major products when the average doping concentration is high. In addition, we observed a MCD signal up to 128 K for the 4% doped clusters (Figure 3c). The decrease of the MCD amplitude with increasing temperature can be fitted well with a Brillouin eq (Figure 3d). This provides another strong evidence that the origin of the magneto-

DOI: 10.1021/jacs.5b07888
J. Am. Chem. Soc. 2015, 137, 12776−12779

optical activity is the exchange coupling between the semiconductor charge carriers and the spins of the dopant ions.[10d]

In summary, we report a successful magnetic doping of $(CdSe)_{13}$ clusters that produces the smallest dilute magnetic semiconductor. Not only do our results uncover a previously unknown pathway for the nanoscale doping process, but they also improve the understanding of the doped semiconductors at the interface of molecules and quantum dots, which paves the way for future applications of nanoscale spin-based devices.

■ ASSOCIATED CONTENT

Supporting Information

The Supporting Information is available free of charge on the ACS Publications website at DOI: 10.1021/jacs.5b07888.

Details of experimental methods, additional optical spectra, mass spectra, doping concentration analysis, and results from time-decay analysis (PDF)

■ AUTHOR INFORMATION

Corresponding Authors

*thyeon@snu.ac.kr

*gerd.bacher@uni-due.de

Author Contributions

∇These authors contributed equally.

Notes

The authors declare no competing financial interest.

■ ACKNOWLEDGMENTS

We acknowledge the financial support by the Research Center Program of the Institute for Basic Science (IBS-R006-D1) (T.H. and K.K.); the German Research Foundation (DFG) under contract Ba 1422/13 (R.F. and G.B.); and the Center for Advanced Meta-Materials (CAMM) funded by the Ministry of Science, ICT and Future Planning as Global Frontier Project (CAMM-No. NRF-2014M3A6B3063716) (J.S.S.). We thank Dr. Y.-H. Yim for help with the LDI-TOF experiments.

■ REFERENCES

(1) (a) Efros, Al. L.; Rosen, M.; Kuno, M.; Nirmal, M.; Norris, D. J.; Bawendi, M. *Phys. Rev. B: Condens. Matter Mater. Phys.* **1996**, *54*, 4843−4856. (b) Murray, C. B.; Norris, D. J.; Bawendi, M. G. *J. Am. Chem. Soc.* **1993**, *115*, 8706−8715. (c) Lee, J.-S.; Stoeva, S. I.; Mirkin, C. A. *J. Am. Chem. Soc.* **2006**, *128*, 8899−8903. (d) Talapin, D. V.; Lee, J.-S.; Kovalenko, M. V.; Shevchenko, E. V. *Chem. Rev.* **2010**, *110*, 389−458.

(2) (a) Peng, X. G.; Manna, L.; Yang, W.; Wickham, J.; Scher, E.; Kadavanich, A.; Alivisatos, A. P. *Nature* **2000**, *404*, 59−61. (b) Manna, L.; Milliron, D. J.; Meisel, A.; Scher, E. C.; Alivisatos, A. P. *Nat. Mater.* **2003**, *2*, 382−385. (c) Joo, J.; Son, J. S.; Kwon, S. G.; Yu, J. H.; Hyeon, T. *J. Am. Chem. Soc.* **2006**, *128*, 5632−5635. (d) Yu, J. H.; Liu, X.; Kweon, K. E.; Joo, J.; Park, J.; Ko, K. T.; Lee, D. W.; Shen, S.; Tivakornsasithorn, K.; Son, J. S.; Park, J. H.; Kim, Y. W.; Hwang, G. S.; Dobrowolska, M.; Furdyna, J. K.; Hyeon, T. *Nat. Mater.* **2010**, *9*, 47−53. (e) Ithurria, S.; Tessier, M. D.; Mahler, B.; Lobo, R. P. S. M.; Dubertret, B.; Efros, Al. L. *Nat. Mater.* **2011**, *10*, 936−941. (f) Liu, Y.-H.; Wang, F.; Wang, Y.; Gibbons, P. C.; Buhro, W. E. *J. Am. Chem. Soc.* **2011**, *133*, 17005−17013.

(3) (a) Shim, M.; Guyot-Sionnest, P. *Nature* **2000**, *407*, 981−983. (b) Yu, D.; Wang, C.; Guyot-Sionnest, P. *Science* **2003**, *300*, 1277−1280. (c) Talapin, D. V.; Murray, C. B. *Science* **2005**, *310*, 86−89. (d) Mocatta, D.; Cohen, G.; Schattner, J.; Millo, O.; Rabani, E.; Banin, U. *Science* **2011**, *332*, 77−81. (e) Sahu, A.; Kang, M. S.; Kompch, A.; Notthof, C.; Wills, A. W.; Deng, D.; Winterer, M.; Frisbie, C. D.; Norris, D. J. *Nano Lett.* **2012**, *12*, 2587−2594. (f) Dahlman, C. J.; Tan, Y.; Marcus, M. A.; Milliron, D. J. *J. Am. Chem. Soc.* **2015**, *137*, 9160−9166.

(4) (a) Mikulec, F. V.; Kuno, M.; Bennati, M.; Hall, D. A.; Griffin, R. G.; Bawendi, M. G. *J. Am. Chem. Soc.* **2000**, *122*, 2532−2540. (b) Norris, D. J.; Yao, N.; Charnock, F. T.; Kennedy, T. A. *Nano Lett.* **2001**, *1*, 3−7. (c) Pradhan, N.; Goorskey, D.; Thessing, J.; Peng, X. *J. Am. Chem. Soc.* **2005**, *127*, 17586−17587. (d) Wang, F.; Han, Y.; Lim, C. S.; Lu, Y.; Wang, J.; Xu, J.; Chen, H.; Zhang, C.; Hong, M.; Liu, X. *Nature* **2010**, *463*, 1061−1065. (e) Yu, J. H.; Kwon, S.-H.; Petrášek, Z.; Park, O. K.; Jun, S. W.; Shin, K.; Choi, M.; Park, Y. I.; Park, K.; Na, H. B.; Lee, N.; Lee, D. W.; Kim, J. H.; Schwille, P.; Hyeon, T. *Nat. Mater.* **2013**, *12*, 359−366.

(5) (a) Beaulac, R.; Schneider, L.; Archer, P. I.; Bacher, G.; Gamelin, D. R. *Science* **2009**, *325*, 973−976. (b) Bussian, D. A.; Crooker, S. A.; Yin, M.; Brynda, M.; Efros, Al. L.; Klimov, V. I. *Nat. Mater.* **2009**, *8*, 35−40. (c) Fainblat, R.; Frohleiks, J.; Muckel, F.; Yu, J. H.; Yang, J.; Hyeon, T.; Bacher, G. *Nano Lett.* **2012**, *12*, 5311−5317. (d) Ochsenbein, S. T.; Feng, Y.; Whitaker, K. M.; Badaeva, E.; Liu, W. K.; Li, X.; Gamelin, D. R. *Nat. Nanotechnol.* **2009**, *4*, 681−687. (e) Awschalom, D. D.; Flatté, M. E. *Nat. Phys.* **2007**, *3*, 153−159. (f) Pandey, A.; Brovelli, S.; Viswanatha, R.; Li, L.; Pietryga, J. M.; Klimov, V. I.; Crooker, S. A. *Nat. Nanotechnol.* **2012**, *7*, 792.

(6) (a) Erwin, S. C.; Zu, L.; Haftel, M. I.; Efros, Al. L.; Kennedy, T. A.; Norris, D. J. *Nature* **2005**, *436*, 91−94. (b) Bryan, J. D.; Gamelin, D. R. *Prog. Inorg. Chem.* **2005**, *54*, 47−126. (c) Norris, D. J.; Efros, Al. L.; Erwin, S. C. *Science* **2008**, *319*, 1776−1779. (d) Santangelo, S. A.; Hinds, E. A.; Vlaskin, V. A.; Archer, P. I.; Gamelin, D. R. *J. Am. Chem. Soc.* **2007**, *129*, 3973−3978. (e) Du, M.-H.; Erwin, S. C.; Efros, A. L. *Nano Lett.* **2008**, *8*, 2878−2882. (f) Buonsanti, R.; Milliron, D. J. *Chem. Mater.* **2013**, *25*, 1305−1317.

(7) (a) Herron, N.; Calabrese, J. C.; Farneth, W. E.; Wang, Y. *Science* **1993**, *259*, 1426−1428. (b) Vossmeyer, T.; Reck, G.; Schulz, B.; Haupt, E. T. H.; Weller, H. *Science* **1995**, *267*, 1476−1479. (c) Alivisatos, A. P. *Science* **1996**, *271*, 933−937. (d) Kudera, S.; Zanella, M.; Giannini, C.; Rizzo, A.; Li, Y.; Gigli, G.; Cingolani, R.; Ciccarella, G.; Spahl, W.; Parak, W. J.; Manna, L. *Adv. Mater.* **2007**, *19*, 548−552. (e) Soloviev, V. N.; Eichhofer, A.; Fenske, D.; Banin, U. *J. Am. Chem. Soc.* **2000**, *122*, 2673−2674. (f) Kasuya, A.; Sivamohan, R.; Barnakov, Y. A.; Dmitruk, I. M.; Nirasawa, T.; Romanyuk, V. R.; Kumar, V.; Mamykin, S. V.; Tohji, K.; Jeyadevan, B.; Shinoda, K.; Kudo, T.; Terasaki, O.; Liu, Z.; Belosludov, R. V.; Sundararajan, V.; Kawazoe, Y. *Nat. Mater.* **2004**, *3*, 99−102. (g) Wang, Y.; Liu, Y.-H.; Zhang, Y.; Wang, F.; Kowalski, P. J.; Rohrs, H. W.; Loomis, R. A.; Gross, M. L.; Buhro, W. E. *Angew. Chem., Int. Ed.* **2012**, *51*, 6154−6157. (h) Beecher, A. N.; Yang, X.; Palmer, J. H.; LaGrassa, A. L.; Juhas, P.; Billinge, S. J. L.; Owen, J. S. *J. Am. Chem. Soc.* **2014**, *136*, 10645−10653. (i) Evans, C. M.; Love, A. M.; Weiss, E. A. *J. Am. Chem. Soc.* **2012**, *134*, 17298−17305.

(8) Park, J.; An, K.; Hwang, Y.; Park, J.-G.; Noh, H.-J.; Kim, J.-Y.; Park, J.-H.; Hwang, N.-M.; Hyeon, T. *Nat. Mater.* **2004**, *3*, 891−895.

(9) (a) Beaulac, R.; Archer, P. I.; Liu, X.; Lee, S.; Salley, G. M.; Dobrowolska, M.; Furdyna, J. K.; Gamelin, D. R. *Nano Lett.* **2008**, *8*, 1197−1201. (b) Na, C. W.; Han, D. S.; Kim, D. S.; Kang, Y. J.; Lee, J. Y.; Park, J.; Oh, D. K.; Kim, K. S.; Kim, D. *J. Phys. Chem. B* **2006**, *110*, 6699−6704. (c) Suyver, J. F.; Wuister, S. F.; Kelly, J. J.; Meijerink, A. *Phys. Chem. Chem. Phys.* **2000**, *2*, 5445−5448. (d) Beaulac, R.; Ochsenbein, S. T.; Gamelin, D. R. In *Nanocrystal Quantum Dots*; Klimov, V. I., Ed.; CRC Press: Boca Raton, FL, 2010.

(10) (a) Kuno, M.; Nirmal, M.; Bawendi, M. G.; Efros, Al.; Rosen, M. *J. Chem. Phys.* **1998**, *108*, 4242−4247. (b) Vlaskin, V. A.; Barrows, C. J.; Erickson, C. S.; Gamelin, D. R. *J. Am. Chem. Soc.* **2013**, *135*, 14380−14389. (c) Fainblat, R.; Muckel, F.; Barrows, C. J.; Vlaskin, V. A.; Gamelin, D. R.; Bacher, G. *ACS Nano* **2014**, *8*, 12669−12675. (d) Gaj, J. A.; Planel, R.; Fishmann, G. *Solid State Commun.* **1979**, *29*, 435−438.

DOI: 10.1021/jacs.5b07888
J. Am. Chem. Soc. 2015, 137, 12776−12779